RSC Advances

PAPER

View Article Online
View Journal | View Issue

Cite this: *RSC Adv.*, 2014, **4**, 3051

Platinum electrocatalyst supported on glassy carbon: a dynamic response analysis of Pt activity promoted by substrate anodization

Sanja I. Stevanović, Dušan V. Tripković, Vladimir V. Panić,* Aleksandar B. Dekanski and Vladislava M. Jovanović*

In previous investigations the physicochemical state of electrochemically activated glassy carbon (GC) has been found to affect the electrochemical activity of GC-supported Pt particles. It has been assumed that carbon functional groups (CFGs) generated by GC anodization are able to renew the Pt surface through bifunctional catalysis. In order to provide evidence for the intimate electrocatalytic relationship between Pt and anodized GC and reveal the cause of CFG-induced enhancement of Pt activity, the dynamic response of Pt black supported on differently anodized GC is analysed in this paper by cyclic voltammetry (CV) and electrochemical impedance spectroscopy (EIS) in acidic solution. It was found that the capacitive properties of Pt black are not affected by modest GC anodization, but the pore resistance of the Pt layer is considerably affected. Clear evidence for the promoting influence of activated GC (*i.e.*, CFGs) on the Pt desorption capability toward reverse hydrogen spillover at a Pt/CFGs-decorated GC interface in the Pt double layer region is elucidated by both EIS and CV measurements. The extent of GC anodization influences, in a quite similar way, both reverse hydrogen spillover desorption parameters (gained by EIS and CV) and the methanol oxidation rate as it has influence on the parameters describing the particular state of activated GC itself. Namely, the pore resistance of the Pt layer and GC resistance due to the presence of CFGs the highest when GC was moderately anodized, whereas the charge transfer resistance for hydrogen spillover desorption is the lowest. The CFGs of the anodized GC are able to "permeate" the above-applied Pt layer, thus increasing the Pt/CFGs-decorated GC interface responsible for the enhancement of Pt electrochemical activity.

Received 4th October 2013
Accepted 14th October 2013

DOI: 10.1039/c3ra45585h

www.rsc.org/advances

1. Introduction

Platinum-based electrocatalysts have been the subject of numerous investigations aiming to improve the activity in reactions that are the most promising candidates for fuel cells, *i.e.*, hydrogen and methanol oxidation and oxygen reduction. In order to reduce the utilization of precious metals and to gain high level activity, a variety of methods for the synthesis of finely dispersed metal nanoparticles supported on different types of substrates has been presented, mostly involving carbonaceous materials. Platinum combined with other metals has been found to have improved activity through bifunctional or multifunctional catalysis in general.[1,2]

Many different types of high surface area carbons have been tested as supports for Pt-based catalysts. The general finding is that activation of a carbon support improves the Pt activity. Carbon is activated either by oxidation[3,4] or electroactivation,[5] but also by thiolation[6] or nitrogen-doping.[7] Since the carbon activation was followed by Pt deposition by various procedures, the improvement in catalyst activity through activation of the support was believed to be influenced indirectly by the activation, *i.e.*, through the improvement of metal dispersion, reduction of its particle size, *i.e.*, by an increase in active surface area of the catalyst.[5,8] In addition, some authors suggested the direct influence of the activated carbon support. They relied on "strong interactions"[9] and "synergistic effects"[3] between the metal and oxygen-containing carbon functional groups (CFGs) of the support produced by activation, mostly in the case of methanol electroxidation (MEO). It is believed that CFGs lower the CO poisoning of Pt during MEO, either by CO diffusion or dissociative adsorption of methanol.[3] On the other hand, spillover and reverse spillover of adsorbed reaction participants between the native surface and another surface that does not adsorb the active species under the same conditions are well documented in the heterogeneous catalysis of composite materials.[10–12] In the case of activated carbon itself, it has been found that it is able to adsorb more hydrogen as its acidity (CFGs content) is higher for unchanged surface areas, as determined by the Brunauer–Emmett–Teller (BET) method.[13,14]

It appears rather hard to distinguish and investigate the direct participation of the activated carbon substrate in the

ICTM – Department of Electrochemistry, University of Belgrade, Njegoševa 12, P.O. Box 473, PAK 125213 Belgrade, Serbia. E-mail: panic@ihtm.bg.ac.rs

particular reaction from its indirect catalytic influence through the properties of deposited catalyst particles. The two-fold influence of the substrate is especially unclear for carbon-supported Pt. In our previous investigations, it was shown that the activity of Pt electrodeposited onto electroactivated glassy carbon (GC) for MEO could be more than ten times higher in comparison to the catalyst placed onto a non-activated substrate.[15] In order to exclude the indirect influence of the GC state on Pt electrodeposition, a well-defined catalyst layer of commercial Pt black has been applied to electroactivated and non-activated GC.[16] The results indicated that CFGs played a role in the promotion of Pt activity. Further detailed analysis of electrochemical impedance measurements on GC, combined with cyclic voltammetry and morphological changes of GC surface, upon intensification of anodizing conditions, revealed an intrinsic influence of the carbon functionalization and the structure of a graphene oxide (GO) layer on the electrical and electrocatalytic properties of activated GC.[17] While GC capacitance continuously increased with intensification of anodizing conditions, the surface nano-roughness and GO resistance reached the highest values at modest anodizing conditions, and then decreased upon drastic GC anodization due to the onset of GO exfoliation. The activity of the GC-supported Pt catalyst for MEO strictly followed the changes in GC nano-roughness and GO-induced GC resistance. Modest anodizing conditions produce the optimal distance between graphite layers and CFGs content, which resulted in the highest electrooxidation activity of the GC/Pt electrode for MEO. However, a strong and explicit confirmation of intrinsic interaction between carbon support and Pt is still lacking, since all conclusions were brought indirectly – by comparing the electrochemical and morphological properties of GC alone to the MEO activity of the Pt/GC electrode.

In the present study, a step forward in the analysis of Pt–GC interaction is undertaken by dynamic response analysis of Pt black supported on GC in different states of activity using the method of electrochemical impedance spectroscopy (EIS). The EIS characteristics and cyclic voltammetric behavior of the Pt/GC electrodes are correlated. The aim is to check whether the defined state of Pt black is unaffected by the GC state while determining if Pt activity is influenced by GC activation or not.

2. Experimental

Platinum black was applied on polished or electrochemically treated glassy carbon samples (GC, Johnson Matthey, UK). The GC electrode surfaces were refreshed before each application of Pt black by abrasion with emery paper of decreasing grain size followed by polishing with alumina of 1, 0.3 and 0.05 μm particle size. The final cleaning of the GC samples was performed in high purity water in an ultrasonic bath. The electrochemical treatment of the polished GC electrode was performed by anodic polarization for 95 s in 0.5 M H_2SO_4 at 1.2, 1.5, 1.7, 1.85 and 2.0 V *vs.* saturated calomel electrode (SCE), which gave GC_{ox} samples. Before Pt black application, a cyclic voltammogram of GC_{ox} electrode was recorded (potential range −0.4 to 1.2 V, sweep rate 50 mV s^{-1}, except for the polished GC electrode when the range was −0.4 to 1.1 V) in 0.5 M H_2SO_4 solution, to ensure that the GC surface was renewed, clean and free of Pt from the previous experiment.

Pt black (Johnson Matthey, specific surface area 24–29 m^2 g^{-1}) was applied on the GC electrodes in the form of a thin layer from an aqueous suspension prepared by ultrasonic homogenization. The layer was formed by pipetting a volume of the suspension onto a GC disk to give a Pt loading of 20 μg cm^{-2}. The applied suspension was dried at room temperature. In order to provide firm attachment of the Pt black layer to the substrate, the tops of the electrodes were covered with a Nafion® layer. The same volume as that of suspension of 10 : 1 (v/v) mixture of high purity water and commercial Nafion® solution (ethanol solution, 5 mass%, 1100 E.W., Aldrich) was applied and dried in air at 65 °C. The real surface area of platinum deposited, A_{Pt} in cm_{R^2}, was estimated from the hydrogen adsorption/desorption region of the basic voltammogram (integrated part of CV, potential range from −0.02 to 0.15 V *vs.* SCE with a correction for double layer charging/discharging). The real surface area of platinum deposited on GC_{ox} was estimated from the difference between electrode voltammetric charges prior to and after deposition of Pt catalyst, $\Delta Q = Q_{GC_{ox}/Pt} - Q_{GC_{ox}}$.

The reagents used were of p.a. purity and the solutions were prepared with high purity water (Millipore 18 MΩ cm^{-1}). The electrolyte used in all electrochemical experiments was 0.5 M H_2SO_4, purged with purified nitrogen prior to each experiment.

All electrochemical experiments were done at room temperature in a standard three electrodes/three compartment glass cell. The counter electrode was a Pt wire while a bridged SCE was used as a reference one. All the potentials are given *versus* SCE. The experiments were performed using potentiostat/galvanostat VoltaLab PGZ 402 (Radiometer Analytical, Lyon, France) or SP-200 (Biologic SA, Grenoble, France). All electrodes were subjected to electrochemical impedance spectroscopy (EIS) measurements at potentials of 0.3 and 0.6 V. The EIS responses to the input sinusoidal potential of 5 mV rms amplitude were registered in the frequency range between 50 kHz and 10 mHz. The recorded EIS data were analyzed using ZView® software, version 2.6 (Scribner Associates, Inc., Southern Pines, NC, USA).

3. Results and discussion

The cyclic voltammograms (CV) of Pt black supported on GC in different states of activity are presented in Fig. 1. CV responses of far-end cases of the samples investigated in this paper – Pt black supported on non-activated GC (GC/Pt) and on thoroughly anodized GC at 2.0 V ($GC_{ox\text{-}2.0}$/Pt), which have already been presented in a previous investigation,[16] are given in the inset of Fig. 1. The voltammetric currents are normalized per real electrochemical surface area of Pt black. A typical CV response of polycrystalline Pt activated by cycling[18,19] is registered in the potential regions of hydrogen adsorption/desorption (below 0.10 V), OH adsorption and oxide formation (above 0.60 V)/reduction (around 0.55 V_{SCE}, cathodic branch) in all cases. Fig. 1 shows that $GC_{ox\text{-}2.0}$/Pt is the single case in which the response of

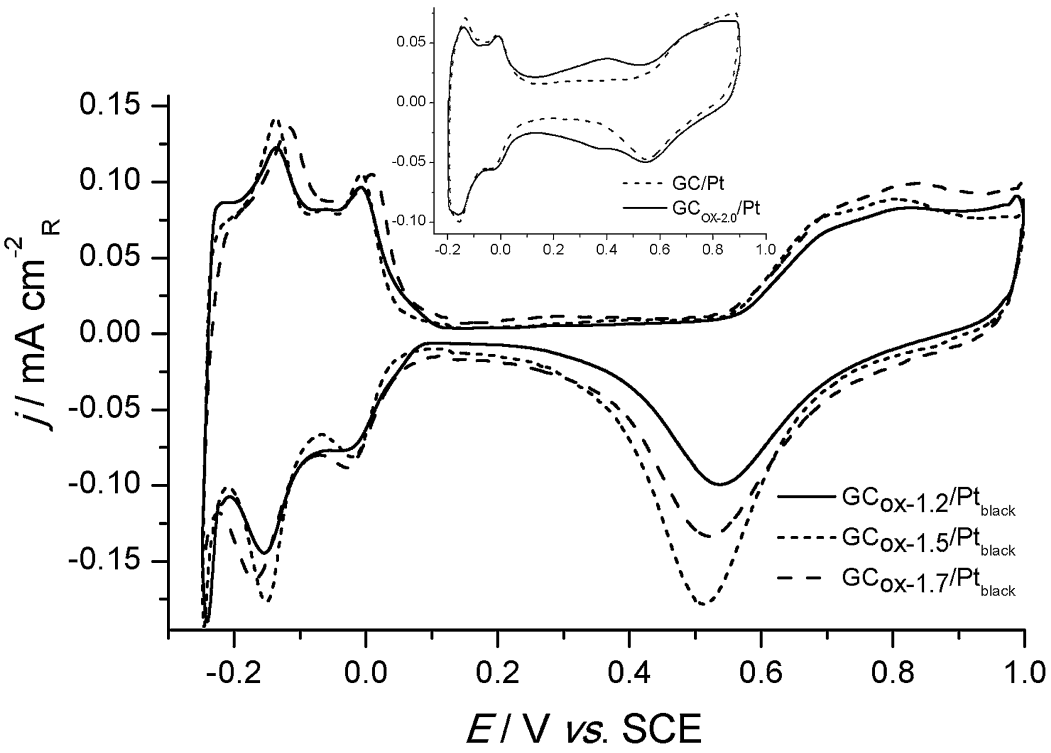

Fig. 1 Cyclic voltammograms of Pt black supported on GC activated for 95 s in 0.50 M H_2SO_4 at 1.2, 1.5 and 1.7 V_{SCE}. Inset: the same on nonactivated GC and that activated at 2.0 V_{SCE}. Pt loading: 20 μg cm^{-2}; electrolyte: 0.50 M H_2SO_4 (25 °C); scan rate: 100 mV s^{-1} and 50 mV s^{-1} for CVs in the inset.

the GC support is clearly seen within the double layer region of Pt. The typical features of weakly and strongly adsorbed hydrogen are found to be slightly affected by the state of GC, whereas OH adsorption and oxide formation/reduction appears to be promoted by GC activation, especially the oxide reduction peak. A similar increase in CV currents is also visible in the double layer region. These effects could be partially caused by the increase in capacitive current of activated GC,[17] onto which the CV features of Pt appear superimposed. The GC_{ox} contribution was, however, subtracted in calculation of Pt real surface area in the potential region of hydrogen adsorption/desorption, and hence this region appears less affected by GC state. Another cause of increased CV current could be related to the morphology of the Pt layer itself. It could differ if the layer were placed on a GC surface of different morphology caused by GC activation.[17] Consequently, the electrochemically active Pt surface area could be different. We reported[16] that an increase in sonication time for Pt water suspensions produces a more compact Pt layer on GC (or GC_{ox})/Pt, which is able to considerably mask the response of GC_{ox} (and consequently its promotion of Pt MEO activity). A more compact layer was also observed to be of larger CV current in the OH adsorption and oxide formation/reduction regions. Fig. 1 shows a similar increase in these CV currents for the samples with moderately oxidized GC that showed the highest promotion of Pt MEO activity ($GC_{ox\text{-}1.5}$/Pt and $GC_{ox\text{-}1.7}$/Pt).[17]

According to the consideration of CV responses (Fig. 1), it follows that both the state of GC and consequently the morphology of the above-applied Pt layer can cause slight changes in the CV current of Pt. However, the magnitude of the changes is too small to explain the registered changes in the activity of the investigated samples for MEO[17] and to distinguish these two possible causes. Following the methodology of the investigations of activated GC itself,[17] the impedance spectra of Pt supported on non-activated GC and GC_{ox} were recorded at 0.30 (the Pt double layer region and GC pseudocapacitive behavior) and 0.60 V_{SCE} (prior to Pt oxide formation) and analyzed. In the case of GC, the impedance data at the mentioned potentials were useful for the elucidation of the relationship between the state of GC and MEO activity of the GC/Pt electrode.[17] The registered spectra for Pt supported on differently oxidized GC are shown in Fig. 2 (symbols), along with the fitting results gained by fitting to equivalent electrical circuit (lines). In relation to the states of GC investigated in previous paper,[17] an additional sample with GC oxidized at 1.85 V was introduced in this paper, since the most pronounced changes in EIS behavior have been registered between GC oxidized at 1.7 and 2.0 V. On the other hand, no substantial difference between GC oxidized at 2.0 and 2.2 V was observed, and hence the latter sample is not the subject of the present investigation. Concerning the state of non-activated GC, there is another modification in this paper. The pre-cycling of GC support is extended from 0.80 (ref. 17) to 1.1 V, since it is required to achieve a stable Pt CV response.

All samples involving GC moderately activated at potentials below 1.7 V exhibit similar EIS features of two indicatively overlapped capacitance loops of a larger diameter at higher

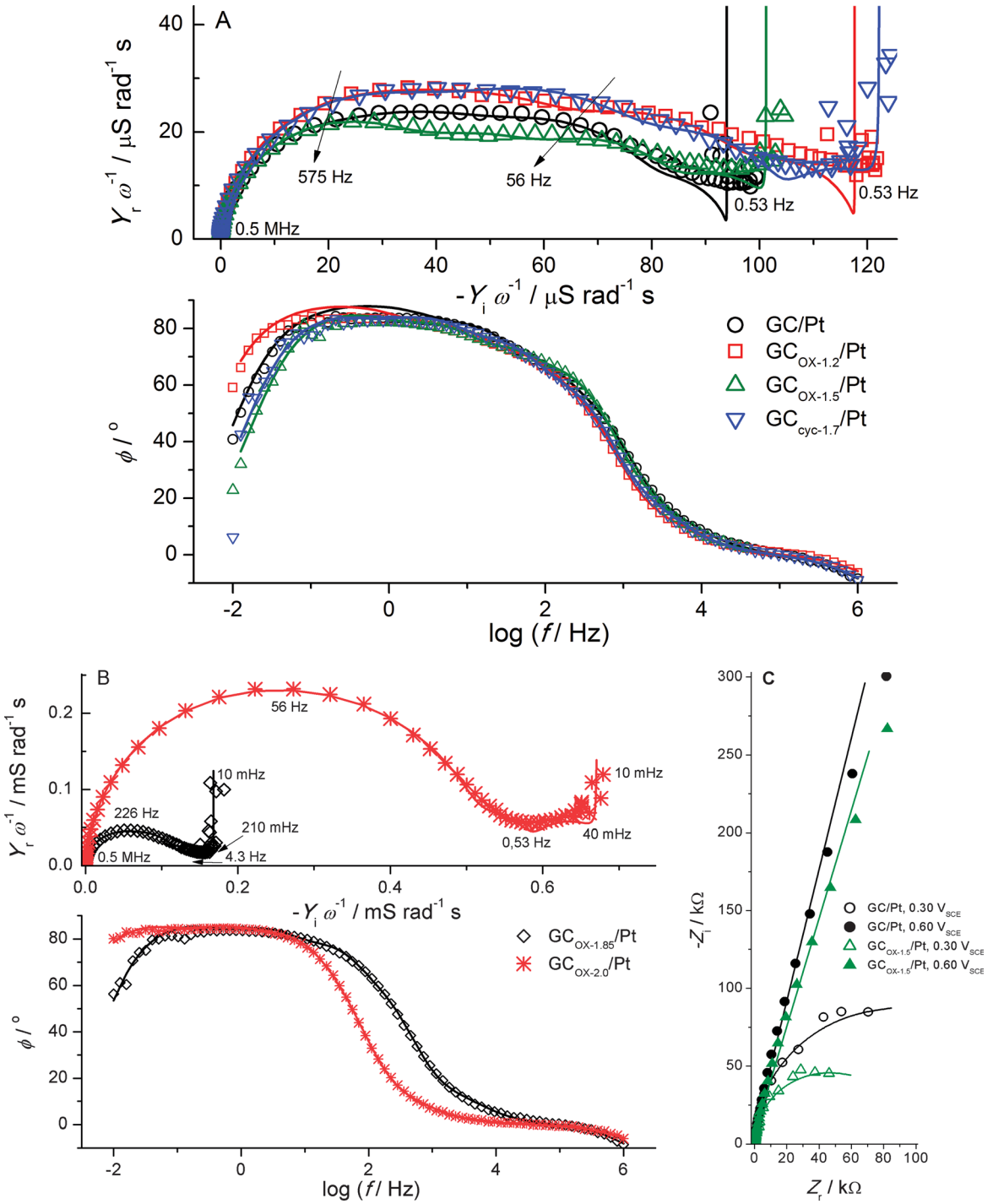

Fig. 2 The capacitance complex plane and phase shift Bode spectra registered at 0.30 V_{SCE} in 0.50 M H_2SO_4 for Pt black supported on differently activated glassy carbon (A and B); (C) illustration of the typical impedance complex plane features at 0.60 in comparison to 0.30 V_{SCE} for the Pt supported on non-activated GC and that activated at 1.5 V_{SCE}; symbols: the EIS data; lines: equivalent electrical circuit data.

frequencies, and several non well-resolved loops of smaller diameter down to 0.53 Hz (Fig. 2A). It appears that each of these loops does not appear considerably and systematically dependent on GC activation. For example, the differences in high frequency domain between $GC_{ox-1.2}$/Pt and $GC_{ox-1.7}$/Pt are almost negligible. However, upon GC activation at 1.85 V, and especially at 2.0 V, the loops at higher frequencies tend to merge and grow considerably (Fig. 2B) with respect to the samples of moderately oxidized GC. It follows that the EIS responses of $GC_{ox-1.85}$/Pt and $GC_{ox-2.0}$/Pt become much more like those of the corresponding GC_{ox} itself presented in previous paper.[17] On the other hand, the responses from Fig. 2A seem almost completely governed by the Pt layer since they are qualitatively different, and the capacitive loops are considerably larger in comparison

to the corresponding GC_{ox} support.[17] These considerations indicate that the EIS response of Pt black in a fairly wide range of frequencies is only weakly influenced by the state of the support.

The unique feature of the EIS response of GC-supported Pt black with respect to the response of the corresponding GC support[17] manifests in low frequency domains: the increase in imaginary capacitance with decreasing frequency for almost constant value of real capacitance. For the samples with moderately oxidized GC (Fig. 2A) this additional feature is seen below 0.53 Hz, whereas it shifts toward lower frequencies for $GC_{ox\text{-}1.85}$/Pt (below 210 mHz) and $GC_{ox\text{-}2.0}$/Pt (below 40 mHz), Fig. 2B. Upon closer inspection of this low-frequency feature at two different steady-state EIS potentials, 0.30 and 0.60 V, it was found to be strictly reserved for the EIS response at the former potential. This is illustrated in Fig. 2C by the impedance complex plane plots of Pt black supported on non-activated GC and that activated at 1.5 V†. Semicircle-like dependences are clearly seen at 0.30 V (also represented by a phase shift sink toward zero at low frequencies in Bode plots, Fig. 2A and B), whereas the samples exhibit a capacitive-like response in the whole frequency domain at 0.60 V. These findings indicate that there is some charge transfer process at 0.30 V that is not taking place at 0.60 V, although these potentials both lay in the double layer region of Pt (Fig. 1), and no net charge transfer process should be expected. In addition, this low-frequency feature at 0.30 V seems to be sensitive to the state of GC support in twofold manner: (1) the semicircle is smaller for the Pt black supported on activated GC (Fig. 2C), which means that GC activation promotes the associated charge transfer and (2) the feature shifts toward lower frequencies upon intensification of GC activation (Fig. 2B). According to the model of the EIS response of porous electrode systems,[20,21] the time constant of EIS features taking place at the inner parts of the porous layer is high (they respond at low frequencies) due to high pore resistance. Hence, the finding (2) induces the conclusion that charge transfer takes place at rather internal parts of the Pt layer, or possibly at those in intimate contact with GC.

In order to quantify the above-mentioned EIS features, the registered data were fitted to equivalent an electrical circuit (EEC). Having in mind the porous nature of a Pt layer and the expected imposition of GC support features in parallel to EIS features of Pt layer, a transmission line model of EEC has been applied.[21,22] The best fittings have been achieved with a five- and six-branch transmission line for the data obtained at 0.60 and 0.30 V, respectively. Chi-squared calculated, based on a modulus, was below 0.009, while the relative error of the parameter values of the EEC elements did not exceed 26%. The additional branch for the data at 0.30 V was required to accommodate the charge transfer resistance. It is to be noted that the EIS data of all samples showed some inductive features at the frequencies above 100 kHz, which is seen in Bode plots of Fig. 2 as a positive deviation of the phase shift. In order to take into account this inductive behavior, a resistor and inductor in parallel were required in series in the transmission line. The parameters of these two circuit elements were found to be independent of the GC state and applied steady-state potential, which indicated that they should be assigned to the measuring system. Anyhow, these elements were taken into account only with the purpose of achieving good fitting quality and to gain more reliable values of the parameters of the transmission line.

The values of the transmission line parameters at two steady-state potentials of 0.30 and 0.60 V are shown in Fig. 3 and 4, respectively, as distributed capacitance, C_D, and resistance, R_D, in the function of the state of GC support. Fig. 3A and, to some extent, Fig. 4A, depicts a negligible dependence of C_D on the state of GC for a moderately oxidized substrate. The capacitance values of the outer parts (closer to the top) of the layer are around 25 μF at both 0.30 and 0.60 V, which indicates their preferential origin in double layer capacitance of Pt, since the corresponding values of GC substrate are considerably lower.[17] For the samples with much more intense oxidation of GC, $GC_{ox\text{-}1.85}$/Pt and $GC_{ox\text{-}2.0}$/Pt, the capacitance values are higher, especially for the latter, as was already indicated in Fig. 2. This increase with respect to the samples with moderately oxidized GC is more pronounced at 0.30 V, as it has also been registered for the GC itself,[17] which demonstrates the considerable contribution of the substrate to the capacitance values of the sample. The substrate remarkably contributes to the capacitance throughout the Pt layer, even to its most outer parts. It follows that either the Pt layer does not completely cover the substrate or the layer forms a highly indented structure causing relieved access of the electrolyte to the substrate. This can induce a joint Pt–GC capacitive response throughout the transmission line.

Substantial differences between the distributed capacitance gained at 0.30 and 0.60 V concerns the changes in capacitance values going from the top toward the bottom of the Pt layer, irrespective of the state of GC. At 0.30 V (Fig. 3A), the capacitance decreases, whereas at 0.60 V (Fig. 4A) it seems rather increased, especially at the most inner parts of the layer (*i.e.*, in the vicinity or at the Pt/GC interface) and especially for the samples of moderately oxidized GC. This brings the discussion back to the involvement of a charge transfer process at 0.30 V (Fig. 2C), which was supposed to take place at those parts of the samples with intimate contact between Pt and GC (Pt/GC interface). It appears that the capacitance of these parts of the layer is lower in comparison to the capacitance of the outermost parts of the layer due to the presence of the species taking part in charge transfer processes. Indeed, as the GC support is more active and production of carbon functional groups (CFGs) is abundant,[17] the decrease in capacitance seems like it is "being spread" from the Pt/GC interface toward the outer parts of the Pt layer (Fig. 3A). In addition, for the samples which showed lower MEO activity (Pt supported on non-activated and thoroughly oxidized GC, GC/Pt and $GC_{ox\text{-}2.0}$/Pt),[17] the decrease in capacitance seems sharper in comparison to the most active samples ($GC_{ox\text{-}1.5}$/Pt and $GC_{ox\text{-}1.7}$/Pt). Note that this sharp decrease takes place at the very bottom of the layer in the case of GC/Pt and transfers to around the middle of a layer for $GC_{ox\text{-}2.0}$/Pt. On the

† $GC_{ox\text{-}1.5}$/Pt was chosen for this illustration because this sample showed the highest MEO activity[17] and some EIS difference with respect to other samples with moderately activated GC (Fig. 2A).

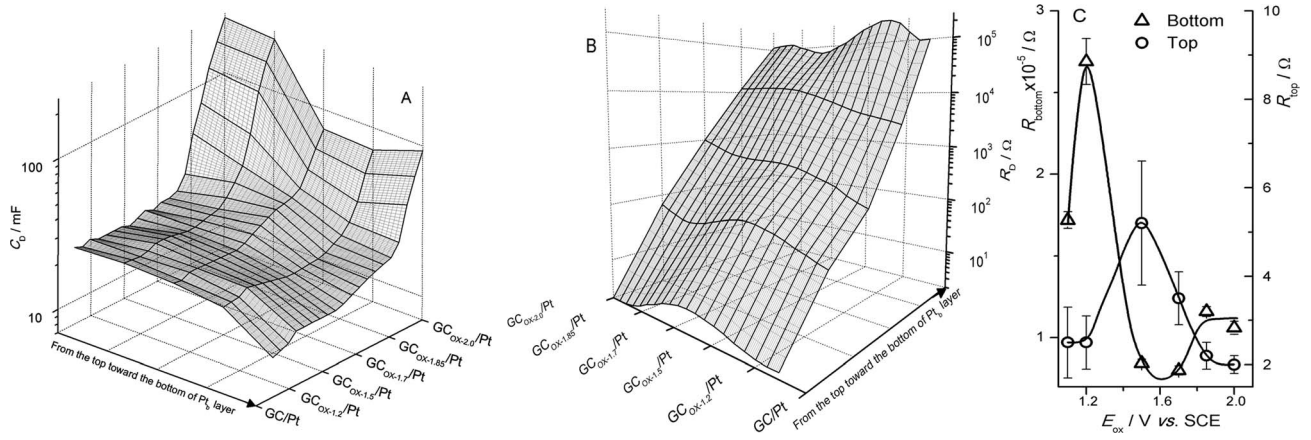

Fig. 3 The distribution of the capacitance (A) and resistance (B) through the electrode assemblies consisting of Pt black (Pt) supported on non-activated and differently activated glassy carbon (GC). (C) The cross sections of the 3D surface (B) at the most outer (top) and inner (bottom) parts of the assemblies with GC activated at different potentials, E_{OX}. Data gained by fitting of EIS data recorded at 0.30 V to transmission line EEC.

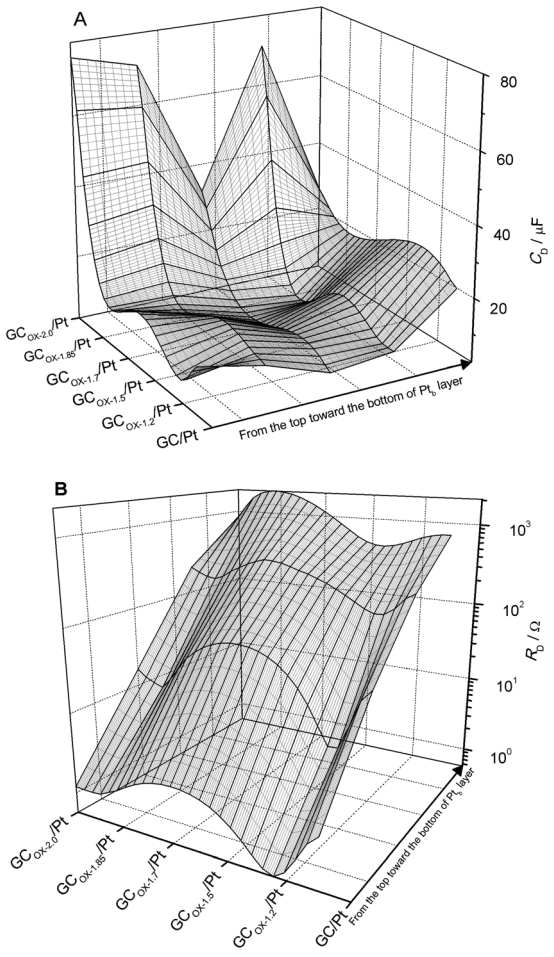

Fig. 4 The distribution of capacitance (A) and resistance (B) through the electrode assemblies consisting of Pt black (Pt) supported on non-activated and differently activated glassy carbon (GC). Data gained by fitting of EIS data recorded at 0.60 V to transmission line EEC.

other hand, the capacitance at the very bottom of the layer gradually increases as the GC activation intensifies. However, one should bear in mind that although decreases in the capacitance through the layer is indicative for the onset of charge transfer, it does not bring the information about its intensity bearing in mind the relationship between the semi-circles of Fig. 2C, which show a lower charge transfer resistance for GC$_{ox-1.5}$/Pt.

The above considerations related to distributed capacitance indicate that a gradual increase in capacitance at the Pt–GC interface (bottom of the layer) with GC activation could have twofold cause. It can be due to gradual contribution of GC as it is being activated, which should produce the capacitance distribution much like that registered at 0.60 V (Fig. 4A), but also due to the growth of Pt/CFGs-decorated GC interface. The former cause apparently dominates in the case of a thoroughly oxidized sample (GC$_{ox-2.0}$/Pt). However, as far as the latter cause is concerned, it should be due to the increase in content of CFGs, but also due to the increase of the GC surface area that "accommodates" the Pt/CFGs-decorated GC interface upon intensification of GC activation.

The distributed resistance, R_D, generally increases considerably from the top toward the bottom of the layer at both potentials (Fig. 3B and 4B), which indicates its close relation to the pore resistance of the layer.[22] However, R_D appears sensitive to the state of GC support. For the outer parts of the layer, R_D shows a maximum for the samples of the highest activity for MEO[1] (see cross-sectioned R_{top} in Fig. 3C). This resembles the behavior of resistance due to the presence of carbon functional groups (CFGs), R_{CFG} (graphene oxide induced GC resistance), registered for GC support.[17] Although the values of R_{CFG} were considerably higher than R_{top}, the position of R_{CFG} within the simple two-branch EEC is the same as that of pore resistance in a transmission line of porous electrode.[17] Hence, it is possible for R_{CFG} to be involved in R_D, with contribution being more pronounced going from the top toward the bottom of the layer. This feature is indicative from R_D at 0.60 V; the maximum is more pronounced in the inner parts of the layer and tends to move toward the samples of thoroughly oxidized GC (GC$_{ox-1.85}$/Pt and GC$_{ox-2.0}$/Pt). For these samples, the position of the domain of electrode assembly abundantly decorated by CFGs was

supposed to be nearer to the GC support than for samples of moderately oxidized support. Similar observations about R_D maximum, although less pronounced, also comes from R_D at 0.30 V, but in this case it does not hold for the very bottom of the layer (R_{bottom} from Fig. 3C) because of the contribution of charge transfer resistance. R_{bottom} values at 0.30 V are two orders of magnitude higher than the corresponding values at 0.60 V (Fig. 4B). This strongly indicates that R_{bottom} is almost completely governed by the charge transfer resistance.

It follows that the CFGs of the oxidized GC substrate is able to "permeate" the above-applied Pt layer, thus affecting its pore resistance and only negligibly its capacitance as illustrated in Fig. 5. As shown in Fig. 5a, rather a low amount of CFGs on the smooth surface of non-activated GC achieve contact with a negligible number of Pt particles. Upon unfolding graphitic ribbons on moderately oxidized GC,[17] Pt particles are "trapped" in a graphene oxide (GO) layer abundantly decorated by CFGs – Fig. 2b. Hence, the permeation effect of CFGs through the Pt layer appears most pronounced for Pt/GC electrode assemblies of modest GC anodizing conditions (Fig. 5b), which also showed the highest MEO activity.[17] As the GO layer is cut off from GC surface roughened by thorough oxidation (Fig. 5c), some Pt particles could be accommodated in micro cavities. Although being in intimate contact with CFGs, these Pt particles are hardly reachable by the reaction species and weakly participate in the reaction. The sketches in Fig. 5 are thus in accordance with the conclusion[17] that, nano-roughness of the GC surface, distance between graphene oxide layers and a CFGs content that reaches the optimal value at modest GC oxidation conditions in order to bring the highest amount of CFGs into intimate contact with the Pt surface, increase Pt activity.

The significant feature in close connection with the Pt–CFGs-decorated GC relationship concerns the appearance of charge transfer resistance (*i.e.*, R_{bottom}) at 0.30 V. The lowest values (*i.e.*, highest activity in a charge transfer process) are obtained for $GC_{ox\text{-}1.5}$/Pt and $GC_{ox\text{-}1.7}$/Pt (Fig. 3C and 5b), which were also of highest MEO activity. In general, GC oxidation causes higher activity of the GC/Pt assembly. In order to analyze further the electrode behavior at 0.30 V, the CV feature within the Pt double layer region has been rechecked in detail. Fig. 6 shows the zoomed anodic double layer (DL) regions of the CVs from Fig. 1.

There is the clear appearance of a so-called "DL peak"[11] (Fig. 6a), which is to be assigned to an additional desorption of H having been reversibly spilt over from the material in intimate contact with Pt. It is believed[23] that hydrogen adsorbed on Pt could be spilt over, *i.e.*, it can migrate from the metal surface toward the carbon support surfaces. This phenomenon has been observed for various amorphous and crystalline substrates, such as oxides, activated carbon, zeolites and metal–organic frameworks.[11] Upon desorption of H from the Pt surface, the H atoms, spill over to the substrate during cathodic scan, migrate back to the freed Pt surface and desorb, which is manifested by the appearance of the DL peak. The appearance of a DL peak has been investigated on a Pt nano-electrode.[11]

It is clearly seen in Fig. 6a that the charge exchanged below the DL peak increases as GC is oxidized more. The curve for the polycrystalline bulk Pt is also given in Fig. 6a to demonstrate the absence of the DL peak. Similarly, the peak cannot be distinguished for $GC_{ox\text{-}2.0}$/Pt because of the appearance of pronounced quinone redox behavior (Fig. 6b). Furthermore, it appears that the quinone peak is suppressed since the Pt layer covers the GC. It is noticeable also in Fig. 6a that the DL peak for $GC_{ox\text{-}1.7}$/Pt shifted anodically, with a position quite close to that of the quinone peak of GC. However, the charge exchanged per surface area is lower in comparison to GC,[17] which indicates the involvement of some other process coupled to a suppressed quinone redox response. It follows that the shift of the DL peak and its collision with the quinone redox behavior appear when GC is oxidized under more drastic conditions, *i.e.*, at the potentials above 1.5 V. As a result, the DL peak cannot be distinguished, while its coupling to the quinone peak causes suppression of the latter. As the quinone peak intensifies upon more drastic anodization of GC, the suppression is less pronounced.

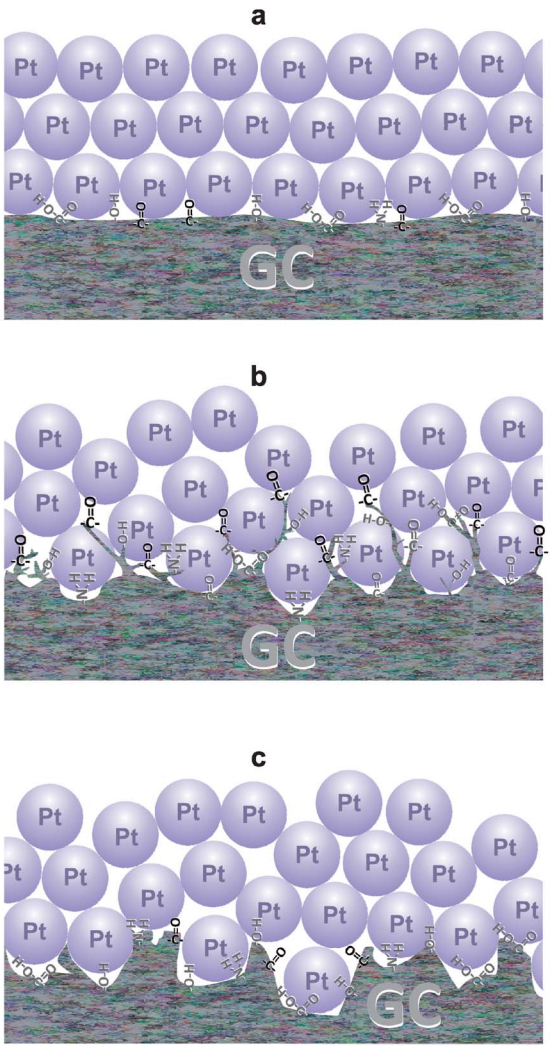

Fig. 5 A schematic of the permeation of the graphene oxide layer abundantly decorated by carbon functional groups through the above-applied Pt black porous layer; (a) Pt on non-activated GC, (b) Pt on moderately activated GC that shows thehighest electrochemical activity and (c) Pt on thoroughly activated GC.

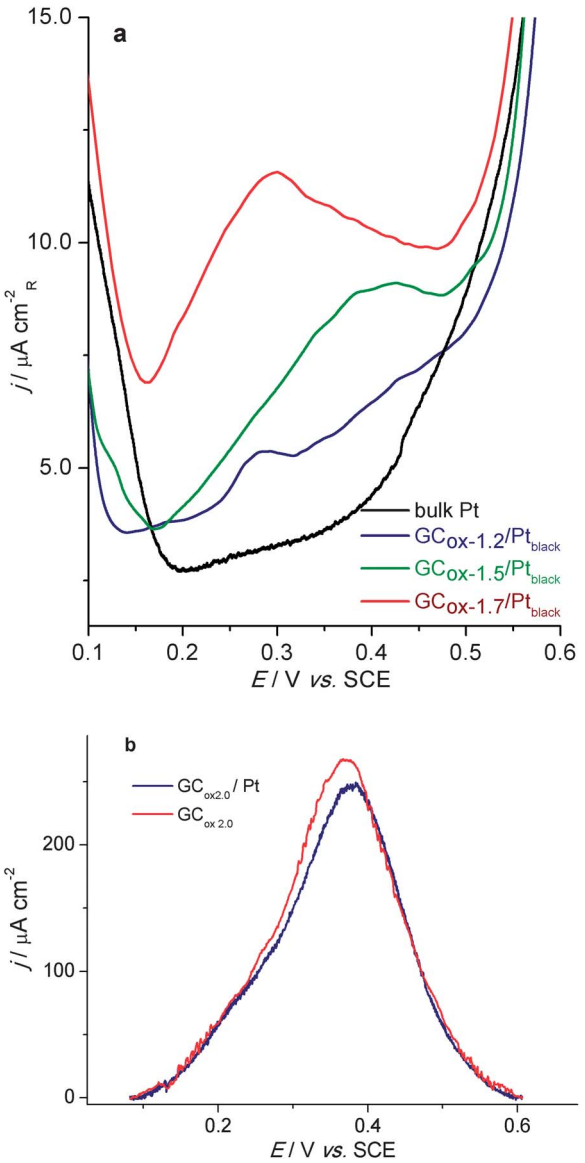

Fig. 6 (a) Details of the anodic parts of CVs presented in Fig. 1; bulk Pt: CV response of the bulk polycrystalline Pt under the same conditions; (b) the same detail of GC$_{ox\text{-}2.0}$/Pt obtained upon subtraction of the CV curve of Pt supported on non-activated GC.

The considerations of Fig. 4 and 6 establish the close connection of the DL peak appearance and the appearance of additional charge transfer resistance at 0.30 V resolved by impedance measurements (R_{bottom} from Fig. 3C). R_{bottom} appears lowest for the GC$_{ox\text{-}1.5}$/Pt and GC$_{ox\text{-}1.7}$/Pt electrode exhibiting the most pronounced DL peak, although for the latter electrode it is not obvious due to merging to the response of the GC substrate. Hence, it is reasonable to assign the charge transfer resistance to the desorption of H atoms having been reversely spilt over from the activated GC surface back to the Pt surface.[10,12] The mechanism is sketched in Fig. 7. The CFGs are able to adopt by spillover the hydrogen primarily adsorbed on Pt, thus setting free the Pt surface. This increases the ability of Pt to adsorb more hydrogen. It can be tentatively assumed that spilt-over H is transferred back to the freed Pt surface by reverse spillover upon anodic desorption of pristine H from Pt. The most intense reverse spillover effect is reserved for the Pt layers supported on moderately activated GC, those which showed the most pronounced permeation effect of CFGs and also the highest MEO activity. This indicates that the general cause of the increased activity of Pt supported on activated carbon (*i.e.*, optimally decorated with CFGs, which makes the largest Pt/CFGs-decorated GC interface) is the ability of activated carbon surfaces to adopt, stabilize and easily release the reaction intermediates, thus enhancing the charge transfer processes on Pt.

4. Conclusion

The electrochemical properties of platinum black supported on glassy carbon (GC) in different states of activity, produced by GC anodization in acidic solution, was investigated in order to elucidate the cause of enhanced activity of Pt supported on optimally activated GC for methanol oxidation (MEO). It has been suggested that it is the nano-roughness of the GC surface, the distance between graphene layers and content of carbon functional groups (CFGs) to reach the optimal value at modest GC oxidation conditions, which induces the highest Pt activity.

It was found that the cyclic voltammetric (CV) behavior of Pt outside the double layer (DL) region is not considerably affected by the state of GC. For thoroughly anodized GC (oxidized at potentials above 1.7 V), the CV features of Pt appear imposed

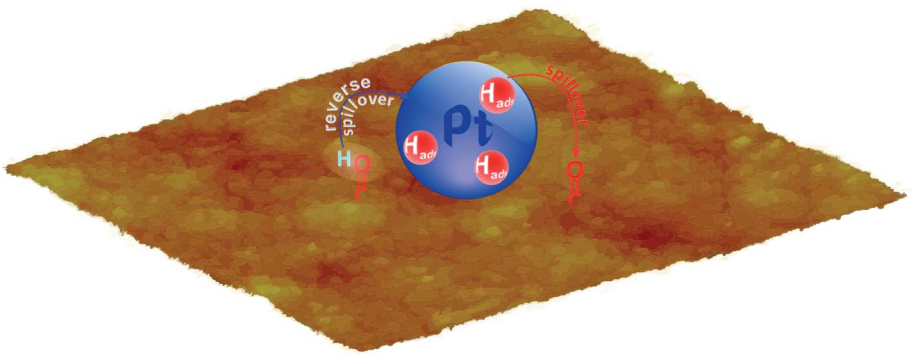

Fig. 7 A schematic of the catalytic interaction of Pt and a graphene oxide layer abundantly decorated by carbon functional groups in reverse spillover of hydrogen natively adsorbed on Pt.

over the CV currents of GC. Impedance measurements show also that distributed capacitance and resistance of a Pt layer is almost insensitive to GC state, unless GC has been thoroughly oxidized when joint Pt–GC distributed capacitive response was registered. However, the appearance of a DL peak was observed for the Pt supported on moderately oxidized GC, assignable to the reverse spillover of hydrogen between substrate and Pt surface. This feature is registered as charge transfer resistance in the impedance measurements.

The analysis of distributed capacitance and pore resistance of the Pt layer indicate that CFGs of the oxidized GC substrate is able to "permeate" the above-applied Pt layer, thus affecting its pore resistance and only negligibly affecting its capacitance. The permeation effect appears the most pronounced for Pt/GC electrode assemblies of modest GC anodizing conditions, which also showed the highest MEO activity. The lowest charge transfer resistance due to reverse spillover of hydrogen is also observed for these assemblies. Thus, CFGs-decorated surfaces of moderately oxidized carbon can adopt, stabilize and easily release reaction intermediates, which is considered to be the general cause of the increased activity of Pt supported on adequately activated carbon.

Author contributions

The manuscript was written through contributions of all authors.

Acknowledgements

This work was financially supported by the Ministry of Education, Science and Technological Development of the Republic of Serbia, Contracts no. ON172060-1.

References

1 A. J. Arvia, A. E. Bolzán and M. Á. Pasquale, Electrochemical Catalysts: From Electrocatalysis to Bioelectrocatalysis, in *Catalysis in Electrochemistry: From Fundamental Aspects to Strategies for Fuel Cell Development*, ed. E. Santos and W. Schmickler, Wiley, Hoboken, NJ, 2011, ch. 8, pp. 249–295.
2 J. S. Spendelow, P. K. Babu and A. Wieckowski, *Curr. Opin. Solid State Mater. Sci.*, 2005, **9**, 37–48.
3 P. Hernández-Fernández, R. Nuño, E. Fatás, J. L. G. Fierro and P. Ocón, *Int. J. Hydrogen Energy*, 2011, **36**, 8267–8278.
4 J. Chen, M. Wang, B. Liu, Z. Fan, K. Cui and Y. Kuang, *J. Phys. Chem. B*, 2006, **110**, 11775–11779.
5 J. M. Sieben, M. M. E. Duarte and C. E. Mayer, *ChemCatChem*, 2010, **2**, 182–189.
6 Y.-T. Kim and T. Mitani, *J. Catal.*, 2006, **238**, 394–401.
7 Y. Zhou, K. Neyerlin, T. S. Olson, S. Pylypenko, J. Bult, H. N. Dinh, T. Gennett, Z. Shao and R. O'Hayre, *Energy Environ. Sci.*, 2010, **3**, 1437–1446.
8 X. Yu and S. Ye, *J. Power Sources*, 2007, **172**, 133–144.
9 H. X. Huang, S. X. Chen and C. Yuan, *J. Power Sources*, 2008, **175**, 166–174.
10 W. C. Conner, Jr and J. L. Falconer, *Chem. Rev.*, 1995, **95**, 759–788.
11 R. T. Yang and Y. Wang, *J. Am. Chem. Soc.*, 2009, **131**, 4224–4226.
12 D. Zhan, J. Velmurugan and M. V. Mirkin, *J. Am. Chem. Soc.*, 2009, **131**, 14756–14760.
13 R. K. Agarwal, J. S. Noh, J. A. Schwarz and P. Davini, *Carbon*, 1987, **25**, 219–226.
14 Q. Li and A. D. Lueking, *J. Phys. Chem. C*, 2011, **115**, 4273–4282.
15 V. M. Jovanović, S. Terzić, A. V. Tripković, K. D. Popović and J. D. Lović, *Electrochem. Commun.*, 2004, **6**, 1254.
16 S. Stevanović, V. Panić, D. Tripković and V. M. Jovanović, *Electrochem. Commun.*, 2009, **11**, 18–21.
17 S. I. Stevanović, V. V. Panić, A. B. Dekanski, A. V. Tripković and V. M. Jovanović, *Phys. Chem. Chem. Phys.*, 2012, **14**, 9475–9485.
18 J. Clavilier, J. M. Orts, R. Gómez, J. M. Feliu and A. Aldaz, *J. Electroanal. Chem.*, 1996, **404**, 281–289.
19 J. Solla-Gullón, P. Rodríguez, E. Herrero, A. Aldaz and J. M. Feliu, *Phys. Chem. Chem. Phys.*, 2008, **10**, 1359–1373.
20 R. de Levie, *Electrochim. Acta*, 1963, **8**, 751–780.
21 Conway, *Electrochemical Supercapacitors – Scientific Fundamentals and Technological Applications*, Plenum Publishers, New York, 1999.
22 V. V. Panić, R. M. Stevanović, V. M. Jovanović and A. B. Dekanski, *J. Power Sources*, 2008, **181**, 186–192.
23 A. J. Robell, E. V. Ballou and M. Boudart, *J. Phys. Chem.*, 1964, **68**, 2748–2753.